University of Southern Indiana
Pott College of Science, Engineering, and Education
Engineering Department

8600 University Boulevard
Evansville, Indiana 47712

# Designing a Deployable Solar Array

Design Report

Brogan Barnes, Kyle Sledge
ENGR 491 – Senior Design
Fall 2023

Faculty Advisor_____ Department Chair_____

# ACKNOWLEDGEMENTS

In this section, we would like to acknowledge USI mechanical engineering staff Dr. Milad Rezvani Rad, Dr. Glen Kissel, Dr. Todd Nelson, and Dr. Julian Davis for their recommendations and support towards the development of this project.

# ABSTRACT

The purpose of this project was to design and develop a deployable solar array for a 3U CubeSat. The motivation for this project was to assist in the advancement of USI's CubeSat technology and future deployment. The objective for the project was to design a deployable solar array for the USI CubeSat project and build a testable prototype. Through literature review, it was determined that a deployable array is most commonly attached to the CubeSat by hinges, and that the deployment sequence must be controlled so the array doesn't damage or disorient the CubeSat. This required that the array either be deployed to a predetermined angle or controlled by a motor once it begins deployment. Previous projects have solved this issue with either a hard stop or latch to keep the array at a specific angle relative to the CubeSat chassis. The team pursued the design and determined the feasibility of a compliant rolling element (CORE) joint to serve as a torsional hinge with a stable position. The CORE joint served as a novel feature of the project since the use of a CORE joint on CubeSats has not been documented. This decision also required the design of a hold and release mechanism (HRM) to both retain the array in a stowed position and initiate deployment. Therefore, the project scope included only the development of the deployment mechanism, not development of solar panels or the CubeSat itself.

# TABLE OF CONTENTS

# TABLE OF FIGURES

# LIST OF TABLES

# LIST OF VARIABLES

$M$: Internal moment of a flexure

$E$: Modulus of Elasticity

$I$: Moment of inertia

$R$: Radius of CORE joint surface

$b$: Base or width of flexure

$h$: Height of flexure

$\sigma$: Bending stress in flexure

$D_f$: Center-to-center distance of CORE surfaces

$R_{DL}$: Distance from contacting cam surface to upper and lower CORE foci

$R_{DU}$: Distance from contacting cam surface to upper and lower CORE foci

$\theta D_f$: Angle between the sides $R_{DL}$ and $R_{DU}$

$\theta R_{DU}$: Angle opposite of $R_{DU}$

$R_U$: Upper cam radius

$R_L$: Lower cam radius

$L_S$: Length of flexure that is straight

$E_L$: Elongation of flexure

$\varepsilon$: Strain in flexure

$L_i$: Initial length of flexure

$\sigma_T$: Stress due to tension

$I_c$: Current

$R_r$: Resistance

$V$: Voltage

$L$: Length of wire

$A_c$: Cross sectional area

$\rho$: Resistivity

$\rho_d$: Density

$V_v$: Volume

$T_0$: Ambient temperature

$T_n$: Surface temperature

$\varepsilon_e$: Emissivity

$\sigma_b$: Boltzmann's constant

$T_{n-1}$: Surface temperature from previous calculation

# 1 INTRODUCTION

A CubeSat is a nanosatellite that has dimensions of 10 cm × 10 cm × 10 cm. This configuration is defined as a 1U CubeSat [1]. The units can be stacked and are commonly designed as 2U, 3U, or 6U. CubeSats are primarily used to either gather data such as temperatures for scientific research or test new technologies before they are adopted by larger spacecraft. Additionally, CubeSat serves as one of the most affordable options to send a satellite to space. These nanosatellites are deployed from either larger spacecraft or the International Space Station and enter low-earth orbit before eventually burning up during re-entry into the atmosphere.

USI's UNITE (Undergraduate Nano Ionospheric Temperature Explorer) team deployed a 3U CubeSat in 2019 with NASA's Undergraduate Student Instrument Program (USIP), shown in an exploded view in Figure 1. The mission of the CubeSat was "to measure plasma properties in the lower ionosphere using a Langmuir Plasma Probe, to measure its internal and skin temperatures to compare with a student-developed thermal model, and to track the orbital decay of the CubeSat, particularly near re-entry" [2]. It was powered by solar panels attached directly to the CubeSat chassis. Sometime after the launch, it was recommended that a deployment mechanism for a solar array be developed for a possible future CubeSat launch. This deployable solar array would result in greater power generation from the solar panels because they would allow for more surface area for solar cells to be attached. More importantly, the array would act as a drag mechanism to assist in the CubeSat's re-entry into orbit, which was an important concern of the UNITE team. An overview of the deployment mechanism is provided in Figure 2.

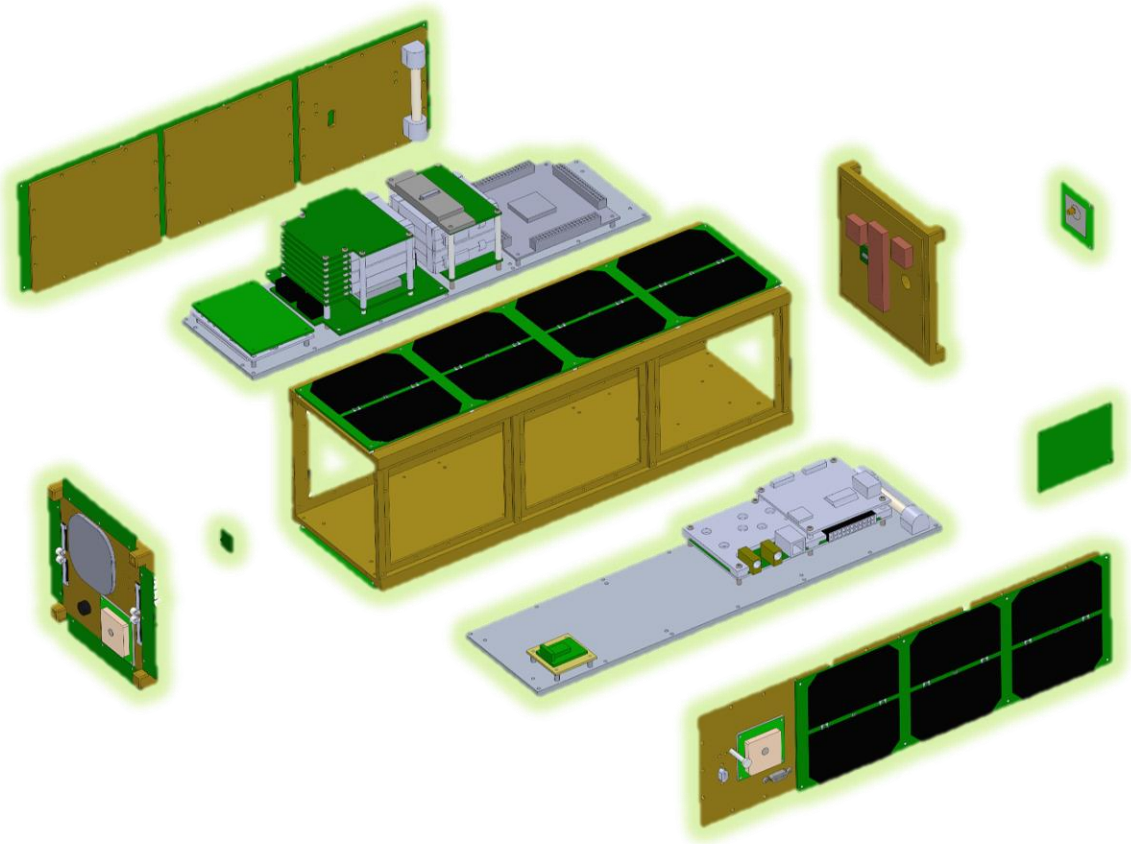

**Figure 1.** USI's UNITE team 3U CubeSat Exploded View [2].

Figure 1 includes all the components developed for the UNITE team's CubeSat. The scope of the deployable solar array project includes only the deployment mechanism of the solar panels, not the solar panels themselves and not any other components of the CubeSat.

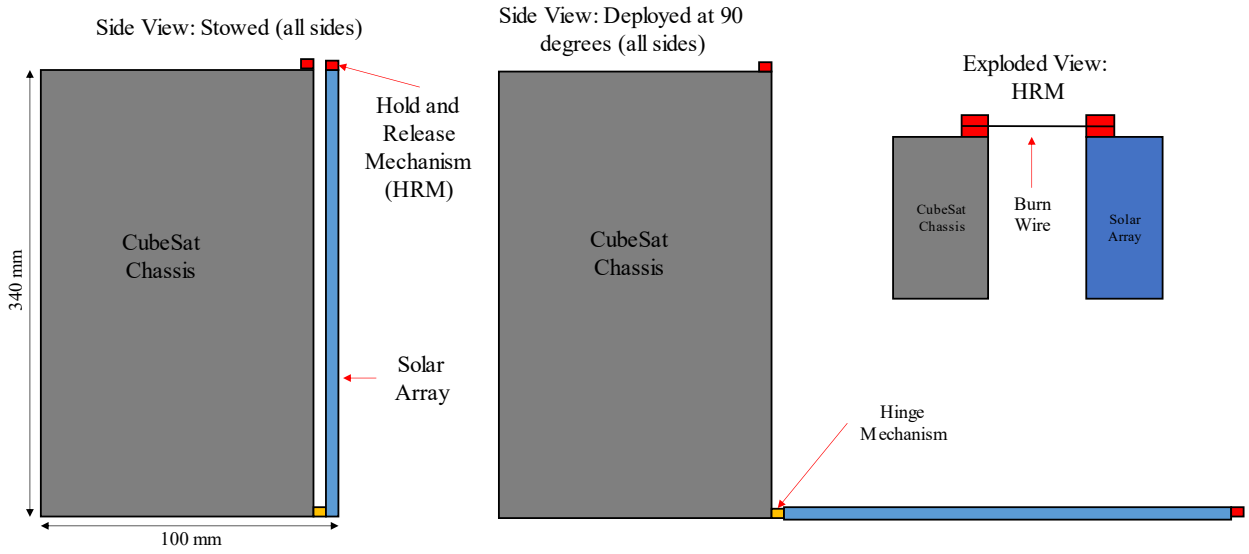


**Figure 2.** Big Picture Overview.

Figure 2 shows both the stowed (left) and deployed (right) configurations of the deployable array. The solar panel is held in the stowed configuration by an HRM and once deployment is initiated, the panel is released from the HRM and rotates about a hinge mechanism. The array is fully deployed when it is oriented 90 degrees relative to the CubeSat chassis, a predetermined angle decided by the team. The array is only required to deploy once and shall remain in the deployed configuration for the remainder of the CubeSat's orbit. Only one side of the array is shown in the figure for simplicity, but the final design would include the mechanisms shown on the remaining three lateral faces. The dimensions of the 3U CubeSat are 340 mm × 100 mm ×100 mm.

## *1.1 OBJECTIVES AND REQUIREMENTS*

The objective of the project is to:

Design a deployable solar array for the USI CubeSat project and build a testable prototype.

The deliverables for the project are as follows:

- Report, Presentation, and Poster

- Design a deployable solar array within CubeSat regulations
- Develop a testable prototype
- Not developing a final model for the CubeSat
- Not developing a CubeSat

The project included seven requirements, listed in Appendix C.

The remainder of this report includes labeled sections and are as follows. Section 2 is the background that includes the motivation and need for the project. Literature review relating to previous and related projects is also included. Section 3 includes the design and construction of the parts necessary for the project. Section 4 is the conclusion that includes a description of what was covered in the report, final notes regarding the project, and future recommendations for the USI UNITE team if they were to implement this deployable solar array in an upcoming CubeSat deployment.

# 2 BACKGROUND

The motivation for this project is to assist in the advancement of USI's CubeSat technology and possible future deployment. The need for the project is a mechanism that shall be connected to a 3U CubeSat chassis and deploy solar panels on the lateral sides of the chassis. This would be an improvement on the UNITE team's previous CubeSat that featured solar cells attached directly to the chassis which allowed much less potential solar cell area and only certain cells to receive solar energy at a given time. USI's previous CubeSat could not have more than one component powered at a time due to the lack of power generation from the solar panels present. A deployment mechanism was requested for a future CubeSat design as it would increase the solar cell area and act as a drag mechanism. The increase in solar cell area would hypothetically increase the power generation allowing a future CubeSat to have less power limitations.

One of the engineering problems associated with the project is the design option of the deployment mechanism. A mechanism must be selected and designed to fit within the dimension and mass regulations of a 3U CubeSat, all covered in the CubeSat design specifications [1]. Another engineering problem is the interfacing between the CubeSat chassis, the deployment mechanism, and the solar panels. The mechanism shall be designed to mate the panels to the CubeSat chassis with both a stowed and deployed configuration. Another engineering problem is the mechanism release and angular position. The mechanism must be able to either maintain a certain angle or vary in angular position by use of a motor. The final engineering problem is designing the mechanism so that it won't damage or release any other components from the CubeSat. A spring-loaded hinge would be a simple design for the mechanism but might damage the CubeSat if it were to deploy with too much torque. Consequently, a spring with too little torque would have trouble keeping the solar panels in the fully deployed configuration unless a type of latching mechanism is considered.

## *2.1 LITERATURE REVIEW*

Multiple literature sources containing similar projects have been reviewed, and three of the sources have been mentioned in detail here. The first piece of literature that included a deployable solar array for a CubeSat was "Development of a Self-Orienting CubeSat Solar Array" [3]. This project was developed to deploy a solar array for a 3U CubeSat that featured a sun-tracking mechanism. The group used the analogy of a sunflower to describe what was the first of nine

project requirements. The deployment mechanism stowed the panels along the top face and each side of the CubeSat, and operated in such a way that it deployed all panels to the same plane. Once deployed, the mechanism holding all panels together was located on the top face of the CubeSat, shown in Figure 3. The deployment mechanism included two Sarrus linkages, a universal joint, and nitinol springs. The linkages gave clearance between the panels and the CubeSat chassis, and the universal joint gave the array the two degrees of freedom that was required for the project. The nitinol springs are Shape Memory Alloys (SMAs), which is a material that can be deformed but will return to its original shape when heated. These springs were given electrical current by static "auxiliary" solar panels located on the opposite end of the CubeSat, also shown in Figure 3 at the bottom of the chassis. When one auxiliary solar panel sensed light, it sent electrical current to certain springs and resulted in the springs contracting and therefore orienting the deployed panels towards the sun.

**Figure 3.** Solar Array in Deployed Position [3].

Figure 3 shows the deployed position of the solar array where the auxiliary solar panels were visible. As stated previously, the auxiliary panels generated electricity so that the nitinol springs could be contracted for the sun-tracking quality of the solar array.

The second deployable solar array project was developed for a scalable solar array built on a 3U chassis that functioned by use of a torsional hinge mechanism shown in Figure 4, Figure 5, and Figure 6 [4]. The results of the project claimed to have five times increase in efficiency of the solar array compared to chassis-mounted solar panels. The solar panels were attached on two of the

lateral sides of the chassis, and each side had a set of three panels for a total of six solar panels, shown in Figure 4. The mechanisms included a main hinge and secondary hinge. The main hinge connected directly to the CubeSat chassis and the secondary hinge connected the remaining solar panels together, shown also in Figure 5 and Figure 6. The hinges were also designed to only allow the array to deploy to 90 degrees relative to the lateral side of the CubeSat. When the array was to be deployed, a fiber that held the array in its stowed position was cut by thermal cutters. This is followed by the cut of a second fiber which then fully deploys the array, shown in Figure 4.

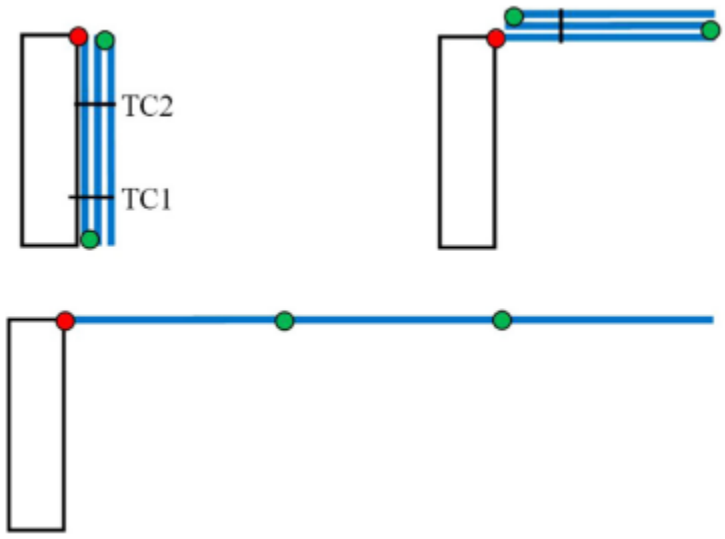


**Figure 4.** Deployment Sequence [4].

Figure 4 shows the deployment sequence of the mechanism and the fully deployed position of the array. The red dot represents the main torsional hinge, and the green dots represent the secondary torsional hinges. The tags TC1 and TC2 represent the fibers that were cut to initiate deployment. Only one side of the array is shown is this figure for simplicity, where the complete array would have the same mechanism on the opposite side of the chassis.

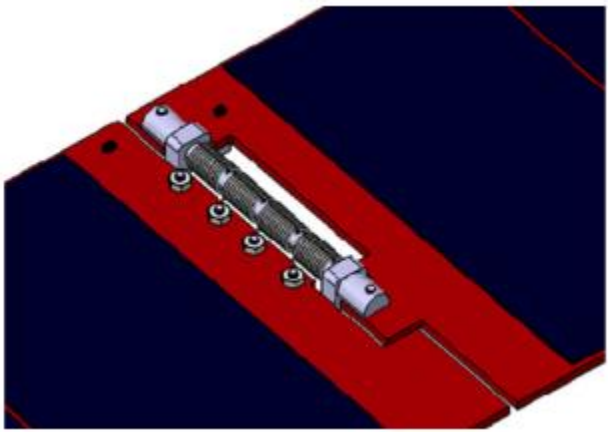

**Figure 5.** Secondary Deployment Hinge [4].

Figure 5 shows the secondary hinge represented by the green dots in Figure 4. There were a total of four secondary hinges for this project.

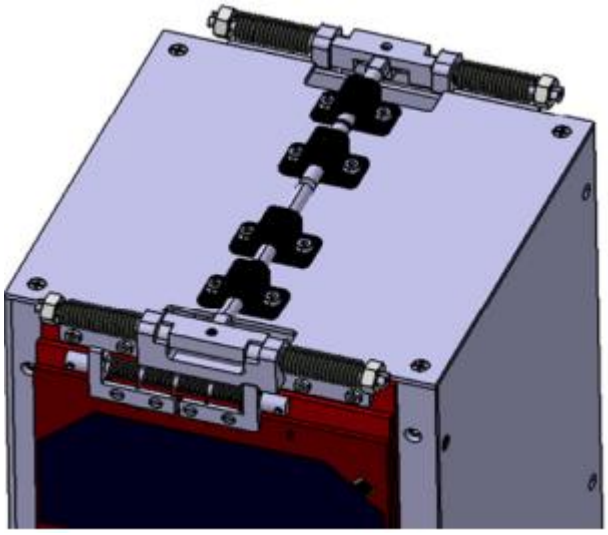

**Figure 6.** Main Hinges Assembly on CubeSat [4].

The next and final project used a pogo pin-based hold and release mechanism to deploy a solar array. This was designed for a 2U CubeSat and would deploy four panels on the four sides of the CubeSat. The panels are held in place by a nylon rope that is tied around a burn resistor connected to a printed circuit board. On the inside and on the end of the panels sits two springs which are compressed when the array is in its stowed configuration. An electrical current is sent through the burn resistor which heats it up enough to burn through the nylon rope that was holding the panels in position. The springs then push off the frame of the CubeSat, deploying the solar array. The panels rotate about a torsion hinge which also acts as a vibrational damper [5]. The torsion hinge

slows the deployment of the solar array. If the solar array deploys too fast, it could damage the hinges and the CubeSat. The model of this CubeSat can be seen in Figure 7. Figure 8 shows the pogo pin-based HRM that can be seen in Figure 7 but in greater detail. Figure 8 can also be found below.

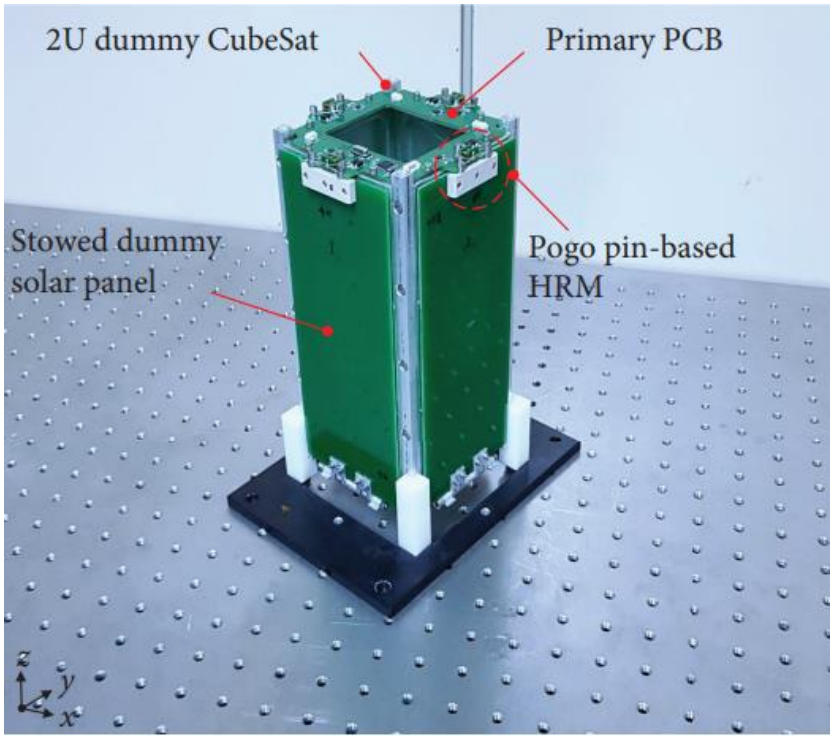


**Figure 7.** CubeSat Stowed Configuration [5].

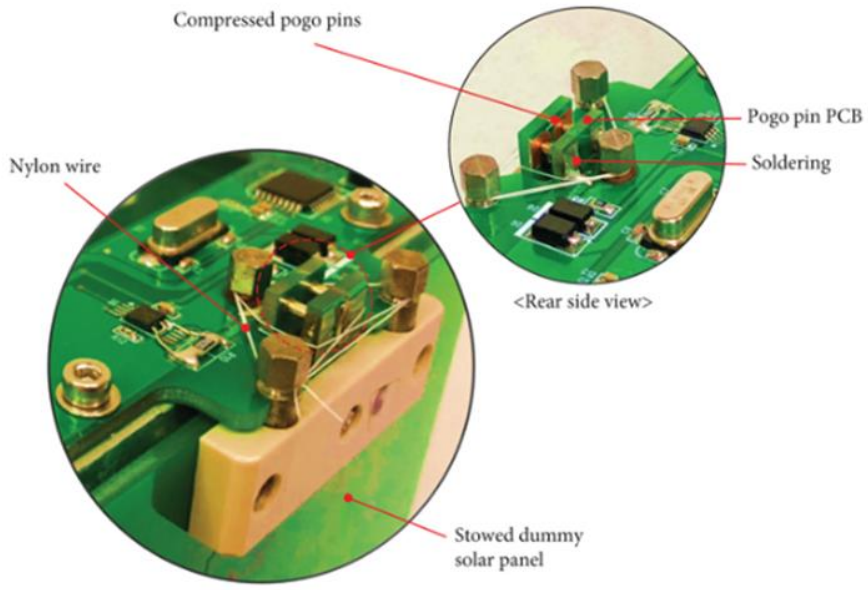


**Figure 8.** Pogo Pin-Based HRM [5].

The next literature that was reviewed included a compliant mechanism. A compliant mechanism is a mechanism that can "gain at least some of their mobility from the deflection of flexible members rather than from movable joints only." [6]. The compliant mechanism described was a compliant rolling element (CORE) joint, shown in Figure 9. The CORE joint functions as a revolute joint that contains two semi-circular surfaces that roll along each other due to the flexures which are visible in black in Figure 9. A CORE joint can have many different surface profiles, but only a circular profile was shown.

**Figure 9.** Assembled CORE Joint [7].

Figure 9 shows the CORE joint in its assembled configuration. The joint contains the stable position shown and the black flexures give the joint its ability to roll 90 degrees to either side of the stable position. The CORE joint has a specific assembly to achieve its rotation, shown in Figure 10.

**Figure 10.** Disassembled CORE Joint [7].

Figure 10 shows the six identical semi-circular parts that are fastened together. The flexures, shown in black, must alternate the sides they are connected to in order to give the joint its ability to function. An optional feature of the CORE joint is the ability to add cams along the surface, shown in Figure 11.

**Figure 11.** CORE Joint with Cams Rotated 90 Degrees [7].

Figure 11 shows the rotational ability of the joint and the cams placed along the surface, in light grey. This figure includes a cam with a flat surface both at the stable position and at the maximum rotated position shown. The flat surface would allow for increased stability at the stable position. This compliant mechanism was reviewed by the team for its potential to serve as a hinge mechanism for the solar array.

## *2.2 WHAT WAS LEARNED*

Thee three projects described above were well-designed and appealing to the team because they all provided unique solutions to the problem the team is interested in. Table 1 shows the key takeaways from the projects. The first project included multiple useful mechanisms for the deployment sequence that were helpful in demonstrating the range of design options. The issue with this project was that it only included virtual models for the solar array. The only physical object was a prototype to test the actuation and reliability of the nitinol springs. A nitinol SMA similar to the one used in this project could be useful but will require further testing and improvement if it were to be used for the team's project.

The second project included a testable prototype that was claimed to have no failures through all operational tests. The use of solar panels connected by torsional hinges in series allowed the CubeSat to have more solar panel area than if the panels were rigidly connected to the chassis. The issue with this project was that during the test, there was no mention of the fiber or the thermal cutters, leaving the reader to wonder if the fiber included in the design was used for testing. Also, the design was claimed to be five times more efficient than chassis-mounted solar panels, but this number was only estimated and never tested. If a mechanism similar to this were to be used for the team's solar array, testing for the thermal cut wire would be critical to determine the reliability of this type of actuation.

The third project, while proven effective, didn't cover the development of the torsional hinges that connected the panels to the CubeSat chassis. Also, if the team pursued a similar solution for the 3U configuration, new knowledge for electrical circuits would need to be learned for the pogo pin-based mechanism. This project did mention two failures modes, both caused by vibrations. The vibration caused by the launch of the CubeSat to space and the vibration caused by the deployable solar array. Vibrations were considered and investigated by the team.

**Table 1.** Comparison of Similar Projects

| | **Key Characteristics** | **Panel Area** | **# Panels** | **Mechanism** |
|---|---|---|---|---|
| **1** | Self-Orienting ability by use of nitinol springs that carried current to allow orientation | ~4(340x100)mm = 136m$^2$ | 4 | Nitinol Springs that carried current. Springs contracted with current flow |
| **2** | Featured a longitudinal stack of panels on two sides of chassis. Deployed by two burn wires. | ~6(326.5x82)mm = 160.6m$^2$ | 6 | Stacked panels (longitudinally) for increased panel surface area |
| **3** | Pogo Pin HRM. Torsional hinge locking mechanism at 90 degrees. | ~4(340x100)mm = 136m$^2$ | 4 | Pogo Pin HRM. Mechanism for specific orientation lock |

Table 1 gives a simple comparison of the most important factors of each reviewed project. After reviewing the three projects, it was found that the first project was the most complex with SMAs and multiple mechanisms to allow sun-tracking, the second project provided high solar panel surface area with few parts, and the third project provided a simple but effective solution.

## *2.3 CONCEPTUAL DESIGNS*

After reviewing multiple previous projects, three concepts were developed, and one was chosen for preliminary design. Multiple factors influenced the final decision and are included in

Table 2 along with the pros and cons of each concept.

The first concept was for a torsional hinge that deployed the panels on all four lateral sides after being released by an HRM, very similar to the third reviewed similar project. This concept is a simple design with a low part count and a solar panel area similar to most 3U deployable solar arrays.

The second concept replaced the conventional torsional hinge with the CORE hinge described in Section 2.1. Although the CORE joint can have many different surface profiles, a circular profile was considered for simplicity and its relation to the literature review. Since the joint contains a stable position, it would eliminate the need for a latch to hold the array at a predetermined angle. This concept would also include an HRM.

The third concept included multi-stage deployment with initiation also from an HRM, similar to the third reviewed similar project. This array seemed very advantageous because it included the highest panel area compared to the other projects. A physical model had also been developed and tested in the literature review. The relative simplicity of this concept is desirable because of the low part count and the fact that new engineering knowledge would most likely not be needed except for the HRM.

**Table 2.** Comparison of Each Concept

| *Concept* | *Pros* | *Cons* | *New Engineering Knowledge Required?* | *Potential Cost* | *Solar Panel Area* | *Simplicity* |
|---|---|---|---|---|---|---|
| ***Torsional Hinge Deployment*** | Simple, effective | Additional mechanism needed for angle lock | Yes for HRM | Low | 136m$^2$ | High |
| ***Compliant Hinge Deployment*** | No lubrication, Stable position | More complicated calculations | " | Low | 136m$^2$ | Low |
| ***Multi-stage Deployment*** | High panel area, Low part count | Additional mechanism needed for angle lock | Yes for thermal cutting | Low | 160.6m$^2$ | Med. |

Table 2 shows the most important takeaways from each concept. After considering these concepts and others from multiple projects, the team has decided to pursue the design of the CORE joint. This was because both team members had recent knowledge and experience with compliant mechanisms, and it would serve as a novel feature of CubeSat solar array deployment. While it requires potentially more calculations, it includes a stable position by design and allows for 180 degrees of rotation that is desired for the project. The other downside to the CORE joint is that it has no retaining quality, which requires an HRM to hold the array in the stowed position. This means that the team will have to obtain new knowledge for designing the HRM.

# 3 DESIGN AND CONSTRUCTION

## *3.1 CORE JOINT DESIGN*

Calculations for the CORE joint were made based upon the available equations in the literature review. The team pursued the design of a CORE joint including a cam, and relevant parameters are provided below.

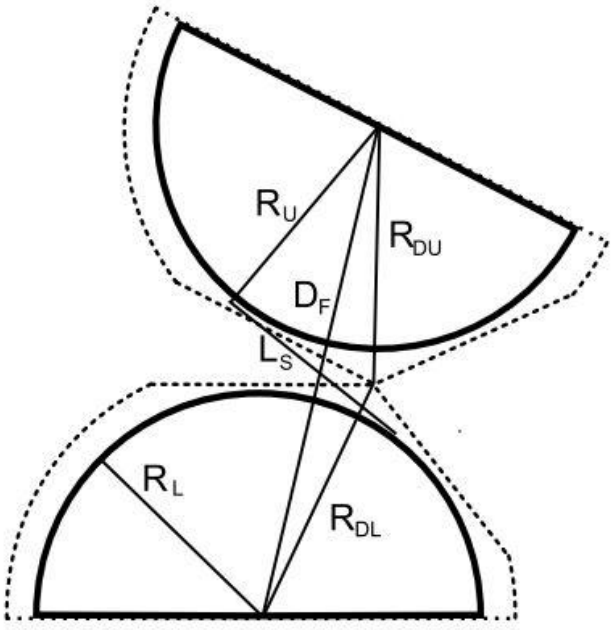


**Figure 12.** Calculation Dimensions [7].

Figure 12 shows the parameters for the calculations performed below. $R_U$ and $R_L$ were selected to be 10 mm. $R_{DU}$ and $R_{DL}$ were selected to be 11 mm.

From these dimensions and the flexure material stainless steel shim stock, described in detail below, the following calculations were made for a flexure thickness based on selected CORE joint radii and flexure length and width.

$$0.06kg \times 9.81m/s^2 = 0.5886\,N \tag{1}$$

$$0.5886N \times \left(\frac{0.3265m}{2}\right) = 0.096N - m \tag{2}$$

Equation 1 is the weight of the solar panel and equation 2 is the max moment of the panel, this would be when the panel is in the fully deployed state at 90 degrees. This moment was set equal

to the moment equation of the CORE joint to find a minimum flexure thickness so the joints could counteract the moment due to the panel.

$$M = \frac{EI}{R} \tag{3}$$

Equation 3 is the internal moment of the flexure where E is the Modulus of Elasticity of Steel (200 GPa), R is the radius of the surface, 10 mm, and I is:

$$\frac{1}{12} b * h^3 \tag{4}$$

Where the b value is 0.00635 m and the h value is to be calculated.

$$0.096N - m = \frac{(200\times10^9)\times\frac{1}{12}\times0.00635mh^3}{0.01m} \tag{5}$$

Equation 5 shows the CORE joint moment equation set equal to the maximum moment due to the solar panel. This gave a thickness of 0.0004m, or 0.008in.

$$\sigma = \frac{Eh}{2R} \tag{6}$$

Equation 6 is the bending stress in the flexure which gave a value of 4 GPa.

$$D_F = \sqrt{R_{DL}^2 + R_{DU}^2 - 2(R_{DU})(R_{DL}) * cos(\theta_{Df})} \tag{7}$$

Equation 7 is used to find the length of $D_F$. $\theta_{DF}$ is unknown and is found using Equation 5.

$$\theta_{D_F} = 180 - \theta_{R_{DU}} - sin^{-1}\left(\frac{R_{DL}}{R_{DU}}\sin\left(\theta_{R_{DU}}\right)\right) \tag{8}$$

Equation 8 includes all known values except for $\theta_{RDU}$, which is found using Equation 6.

$$\theta_{R_{DU}} = cos^{-1}\left(\frac{(R_U+R_L+h)^2+R_{DL}^2-R_{DU}^2}{2*(R_U+R_L+h)R_{DL}}\right) - \theta_1 \tag{9}$$

Equation 9 includes all known values where $\theta_1 = 0$. Plugging in known values gives an angle of 0.384 radians or 22.00 degrees. This value was plugged into Equation 8 to give an angle of 136 degrees or 2.37 radians. This was finally plugged into Equation 7 to give a length for $D_F$ of 0.02040 m or 20.4 mm. From these calculations, the following dimensions and stresses were found.

$$L_S = (R_U + R_L)\sqrt{\left(\frac{D_F}{R_U+R_L}\right)^2 - 1} \tag{10}$$

Equation 10 was used to find the value of $L_S$. All values were now known and gave a length of 0.004 m. From here the elongation of $L_S$ was calculated.

$$E_L = L_S - (R_U + R_L)cos^{-1}(\frac{R_U+R_L}{D_F}) \quad (11)$$

Equation 11 was used to find the elongation of $L_S$ and was 0.000033 m.

$$\varepsilon = \frac{E_L}{L_i} \quad (12)$$

Equation 12 used $E_L$ and the full length of the flexure, $L_i$, to find the strain in the flexure. $L_i$ was approximated to be 0.03142 m. The strain was calculated to be 0.001.

$$\sigma_T = E\varepsilon \quad (13)$$

The strain was used in equation 10 with the Modulus of Elasticity to calculate the stress due to tension, 0.9 GPa.

The flexures for the CORE joint were made from stainless-steel. This material was selected because it has good corrosion resistance and high modulus of elasticity. The surfaces of the joint can be made from plastic such as ABS since it is cost-effective and suitable for space.

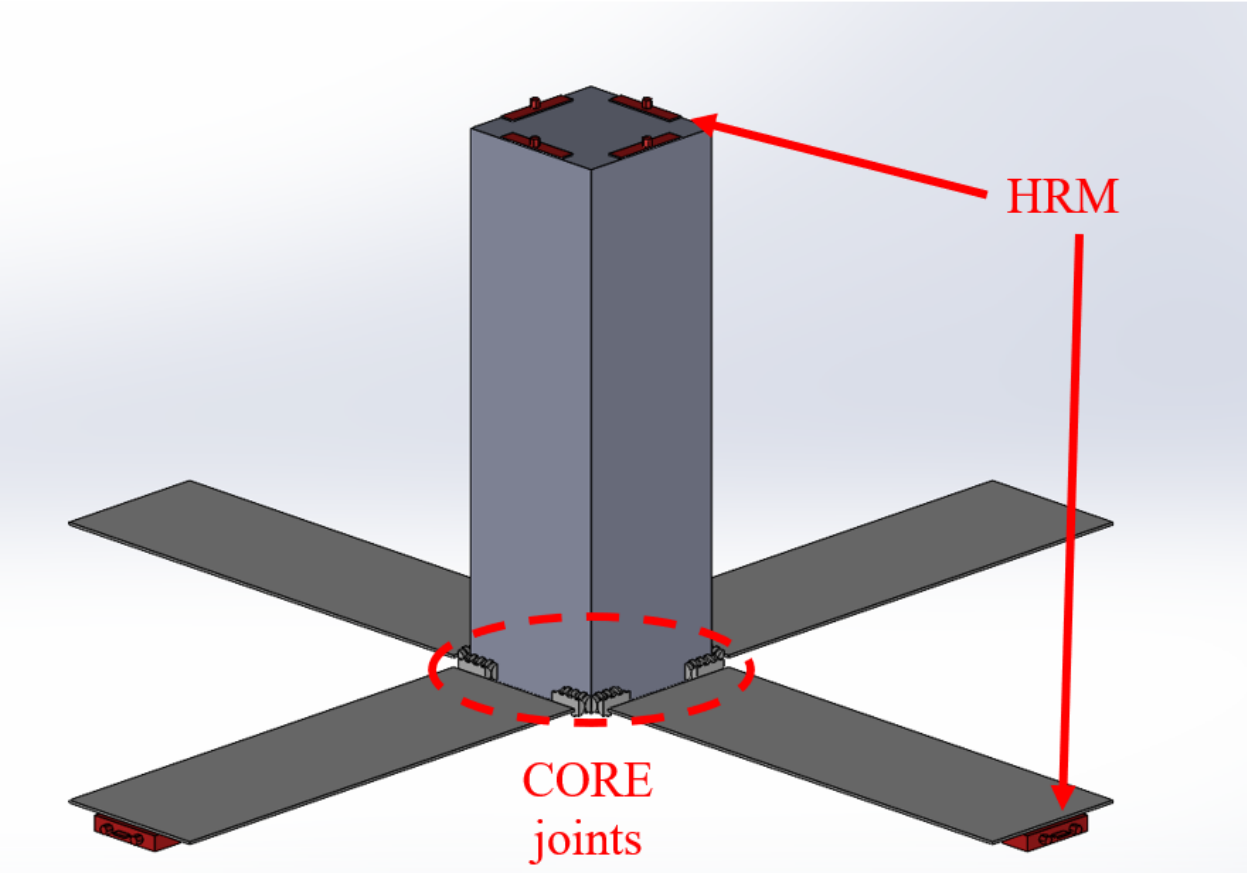


**Figure 13.** Final Design with CORE Joints.

Figure 13 shows the design of the deployment mechanism placed on all lateral sides of the chassis. There are two CORE joints on each face for a total of eight joints. The model shown in Figure 10 has only three flexures, which introduced a slight rotational bias in the CORE joint, visible in Figure 9. This design choice was adapted for the project so that the joints would have a bias to rotate slightly past 90 degrees, and could then be prevented from doing so by the addition of a hard stop. The deployment mechanism was to be tested with a dummy CubeSat chassis and dummy solar panels.

Based on the design choices and calculations, fabrication of the prototype began with 3D printing of the CORE joint surfaces, dummy panels, and dummy chassis. These parts were printed because of the availability of printers on campus, and the designs were cost-effective and allowed for simple design changes. All parts were printed from Polylactic Acid (PLA). The first iteration of the CORE joint utilized a hard stop on the side of the joints so that the mechanism would be prevented from rotating past 90 degrees upon deployment. The surfaces were also designed to

house 1/8” high-temperature neodymium magnets, shown in Figure 14, which were purposed to additionally assist the joints to rotate to and remain deployed at the joint’s center position, 90 degrees relative to the chassis.


**Figure 14.** 1/8” x 1/8” Neodymium Magnet.

These magnets were selected because of their: convenient size to fit within the cams of the CORE joint, high temperature rating of 300°F, and nickel-plated finish for corrosion-resistance. These Grade N38SH magnets had a maximum pull of 1.5lbs each.

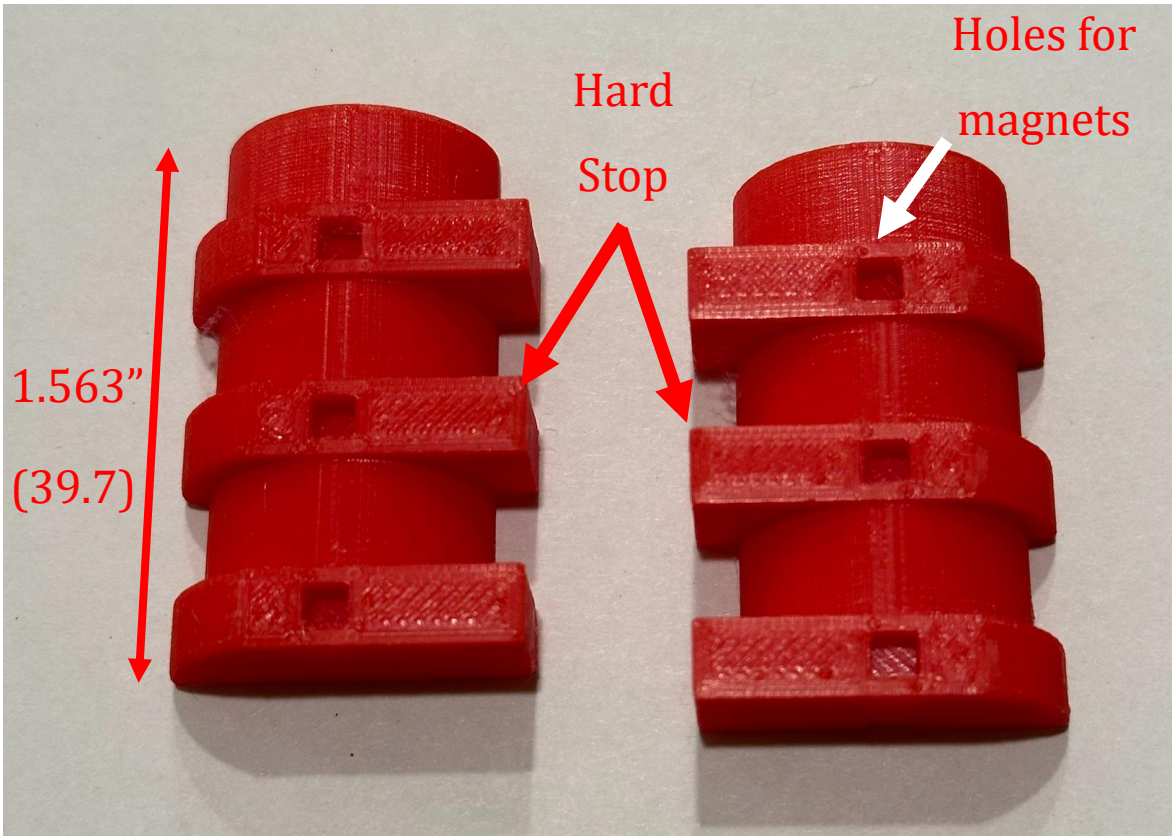


**Figure 15.** First Iteration of CORE Joint Surfaces.

The design of the CORE surfaces in Figure 15 had to be altered, as the CORE joint didn’t function as it was designed to. This is visible in Figure 16 and Figure 17 once the joint was assembled.

**Figure 16.** First CORE Joint Failure.

Figure 16 shows the first assembled joint, and the failure it exhibited. The steel shim flexures were fastened to the joint surfaces, in the same fashion that is visible in Figure 10. The joint didn't rest at the center position but instead at the position shown. The joint could roll along its surfaces but was unable to return to the center position.

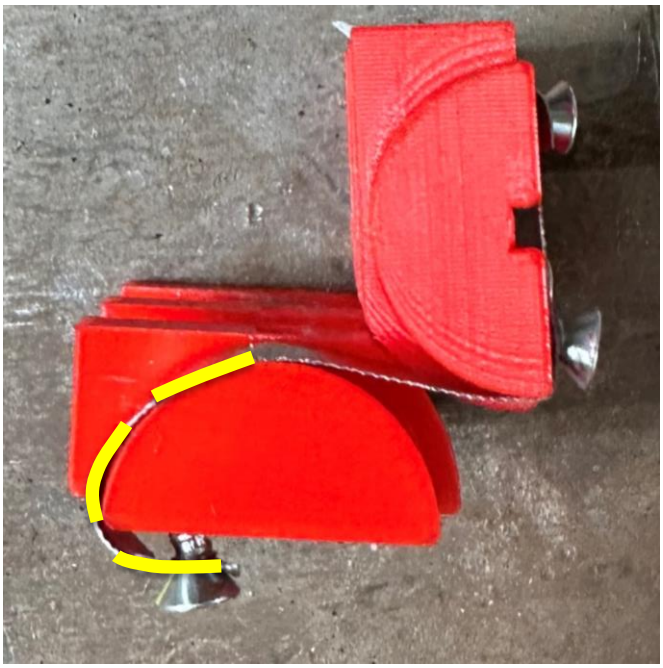

**Figure 17.** First CORE Joint Failure cont.

Figure 17 shows the other position the joint rested at. Instead of behaving as a revolute joint, the CORE joint instead behaved as a mechanism with two stable positions. This unexpected failure was likely due to either the thickness of the flexures or the geometry of the CORE surfaces. After this failure was observed, a second iteration of the CORE joint was made in an effort to resolve the issue. This solution involved the flexures being incident to a constant radius. This differs from the first iteration where the flexures were fastened to the flat side of the joint, resulting in a non-constant radius, highlighted in yellow. This was important because a non-constant radius can result in stable positions, as found from this iteration.

The updated design of the CORE joint featured a constant radius for the flexures once they were fastened to the surfaces. This change was made to alleviate the stable positions exhibited in the first iteration of the joint.

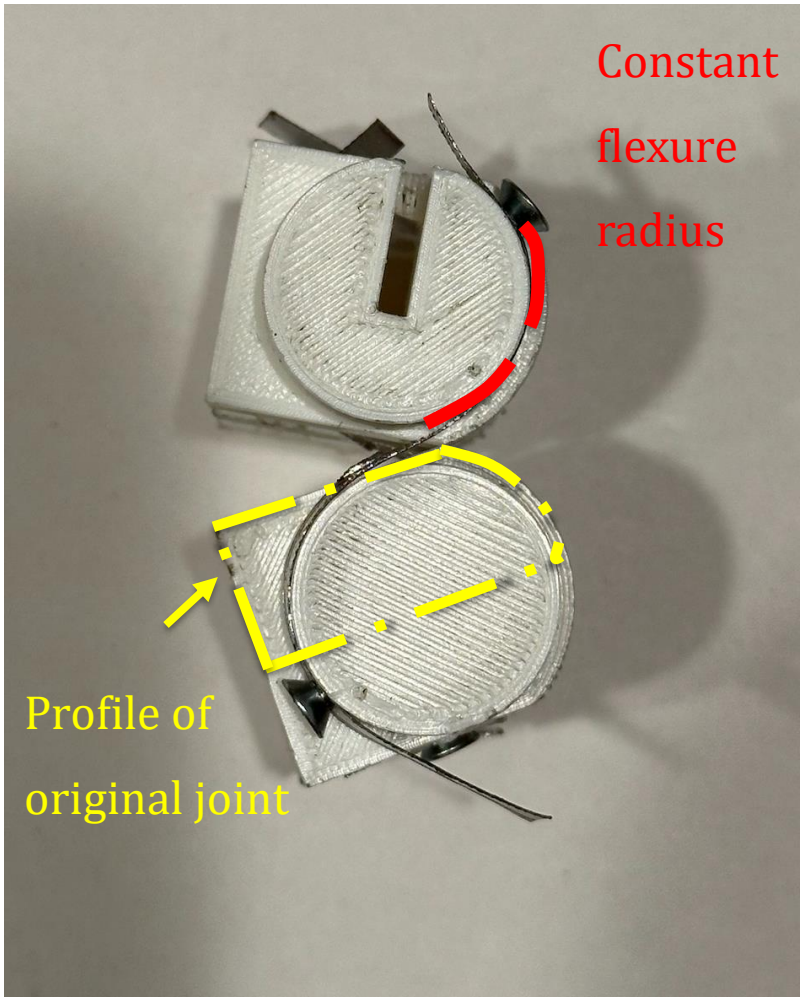


**Figure 18.** Second CORE Joint Failure.

The second CORE joint in Figure 18 resulted in the same failure as the first joint, even with a constant flexure radius, highlighted in red. This joint also didn't rest at the correct center position and exhibited stable positions. All critical dimensions were the same as the first iteration, except the thickness of the joint. The design of this joint mirrored the original joint along the flat surfaces, the profile of the original is shown in yellow. This change allowed for the constant flexure radius.

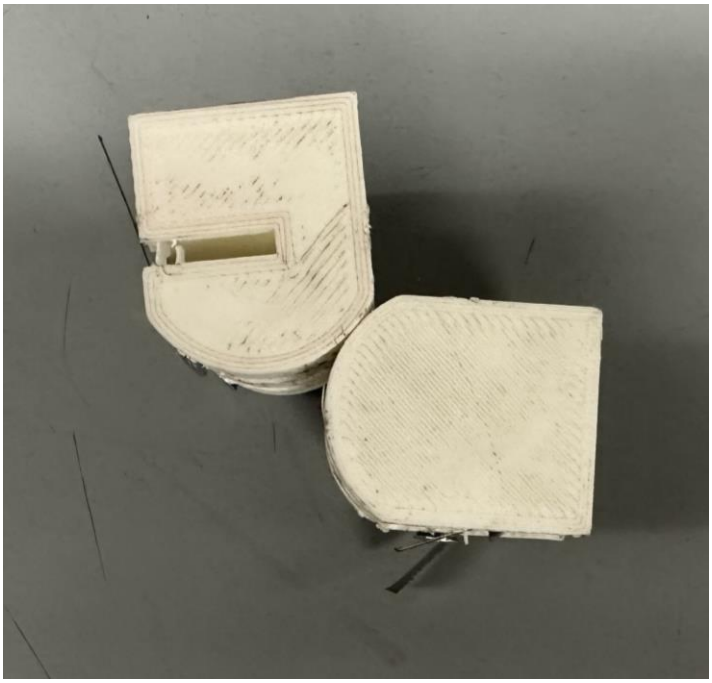

**Figure 19.** Second CORE Joint Failure cont.

Figure 19 shows the other stable position observed by the team. Following the repeated failures of the CORE joints, it was determined that the CORE joint was not feasible as a novel feature of CubeSat solar array deployment. This was because of the ability it lacked to function with flexure thicknesses greater than typical designs (~0.001”). The team decided on a different mechanism to meet their project requirements, opting for an aluminum frame torsional hinge.

## *3.2 TORSIONAL HINGE TESTING*

The torsional hinge selected was available on the McMaster-Carr website, with basic dimensions shown below in Figure 20. A hinge with holes was selected so that it could easily be fastened to the dummy CubeSat panels and chassis with socket head cap screws. The torsional hinge was selected by the team for the reasons listed below:

- Previously tested and used in multiple CubeSat deployable solar arrays (two described in literature review)
- Available in convenient sizes
- Cost-effective (see Appendix B)
- Features a resting position at 90 degrees

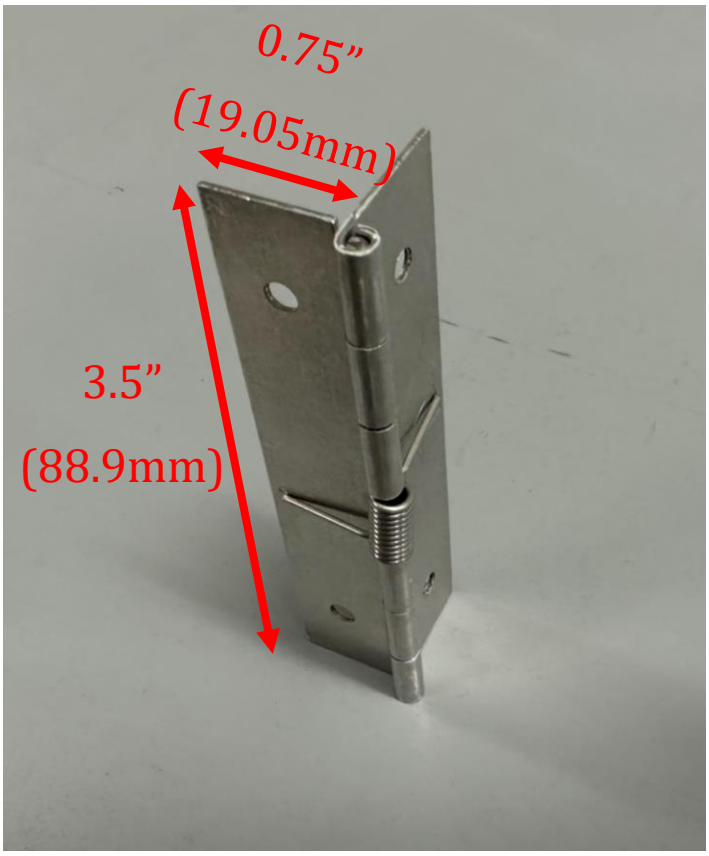


**Figure 20.** Torsional Hinge Selected for Prototype.

The torsional hinge was proven successful through 20 deployment tests with no observed issues, that is deploying from the stowed position along the lateral face of the CubeSat to 90 degrees relative to the same face. The tests were performed in both the vertical orientation and the horizontal orientation shown in Figure 21.

**Figure 21.** Torsional Hinge Testing Assembly in Horizontal Orientation.

The tests were performed in these orientations to prove the functionality of the hinge both with and without assistance from gravity. While the vertical tests resulted in greater vibrations in the panel than the horizontal tests, no damage to any parts was noticed.

## 3.3 *HRM DESIGN*

The hold and release mechanism chosen by the team is similar to the projects covered in Section 2.1. It consists of a nylon rope that will be melted and cut by nichrome burn wire once electric current is applied. This HRM was chosen due to its lightweight and simplistic design. This type of HRM has also been tried and tested as a trusted way to deploy components from a CubeSat. In Figure 22 below the HRM can be seen.

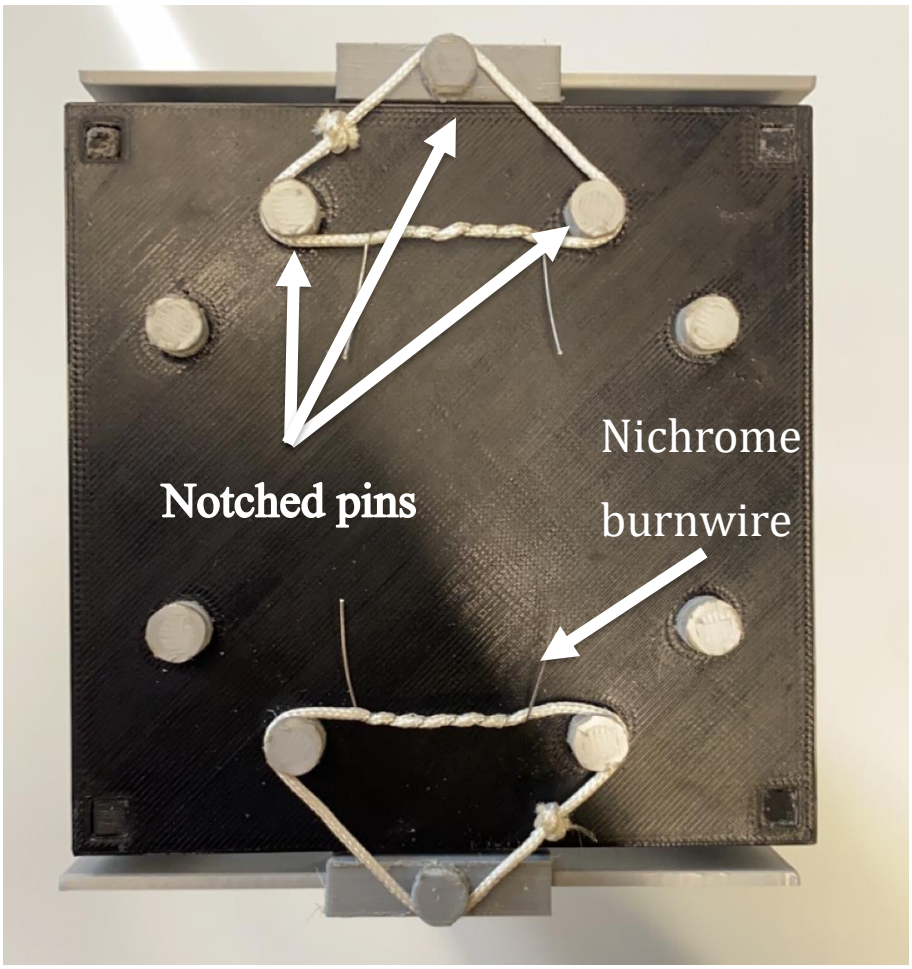


**Figure 22.** Nylon Rope & Nichrome Burn Wire.

The nylon rope was chosen due to its low melting point, moderate strength, and availability [8]. It is strong enough to hold the solar array in the stowed configuration without risk of tearing or breaking. Its low melting point allows the nichrome burn wire to melt or cut the nylon at low temperatures. This is beneficial as it takes more power for the nichrome wire to reach higher temperatures. The nichrome wire was chosen due to its high resistivity and availability [9]. Materials with high resistivity dissipate more heat with less power.

The nichrome burn wire rising in temperature due to power from an electrical current is known as Joule Heating, also referred to as resistive heating. The final temperature of the nichrome burn wire was calculated by considering the net energy within the wire. Where the net energy is heat energy, energy in is from Joule Heating, and energy out is from convection and radiation [10].

$$E_{net} = E_{in} - E_{out} \tag{14}$$

$$E_{in} = I^2 R(t) \tag{15}$$

$$E_{net} = c\rho V(T_n - T_0) \tag{16}$$

$$E_{out} = hA_s(T_{n-1} - T_0)(t) + \sigma\varepsilon A_s(T_{n-1}^4 - T_0^4)(t) \tag{17}$$

The energy equation was simplified to solve for $T_n$, the final temperature of the nichrome burn wire. Multiple assumptions were made in order to solve for the final temperature. One of which being that there is no convection occurring as the CubeSat and subsequently the HRM mechanism will be in the vacuum of space. The power going into the nichrome burn wire was also assumed to be ocurring at a constant rate. In reality as the nichrome heats up the amount of power going into the wire will change because the nichrome has higher resistivity as the temperature rises. This change in power can be best explained by Ohm's Law and the effects of resistivity and resistance. Ohm's Law can be seen in Equation 18 and resistance can be seen in Equation 19 below.

$$V = IR \tag{18}$$

$$R = \frac{\rho L}{A_c} \tag{19}$$

CubeSats are powered by batteries and so will the HRM. Batteries act as constant voltage sources, this means the battery will produce the same voltage regardless of the change of current and resistance in the system. So as the resistivity and subsequently the resistance rises this means the current must decrease. As seen in Equation 15, if the current decreases, then so does the energy going into the nichrome burn wire. The team believes that this assumption of constant power is within reason for the calculations as the resistivity of nichrome only varies from four to six percent all the way up to its melting point [11]. The length of nichrome wire and its thickness also affect the resistance of the system. The length and thickness of the nichrome wire were chosen for ease of use and to keep the resistance low. The chosen length was four inches, and the thickness was

30 gauge. The heating of the wire was assumed to be uniform with no temperature gradient across the length of the nichrome wire. The last assumptions made were those concerning the initial conditions of the system. The initial temperature of the wire and the temperature of its surroundings were both assumed to be at 0°C. This is based off studies and research stating that CubeSats usually operate in 0-20°C conditions [12]. Now Equation 15, 16, and 17 were substituted back into Equation 14 and $T_n$ was calculated using the assumptions stated. The final equation can be seen below.

$$T_n = \frac{\left(I^2 R(t) - \sigma \varepsilon A_s \left(T_{n-1}^4 - T_0^4\right)(t)\right)}{c\rho V} + T_{n-1} \tag{20}$$

Equation 20 was iteratively calculated using excel. Every .01 seconds the equation was calculated, all the way up to 10 seconds. A graph was made to be able to visually see the increase in temperature with respect to time given the amount of power sent through the nichrome wire. The graph can be seen in Figure 23 below. The CubeSat will have a limitation on how much power it can provide to the nichrome wire so Equation 20 was calculated a number of times to see what the lowest amount of power is required for the nichrome wire to exceed the nylon melting point. It was concluded that a minimum of 1.5W be provided to the wire to insure it will melt or cut the nylon.

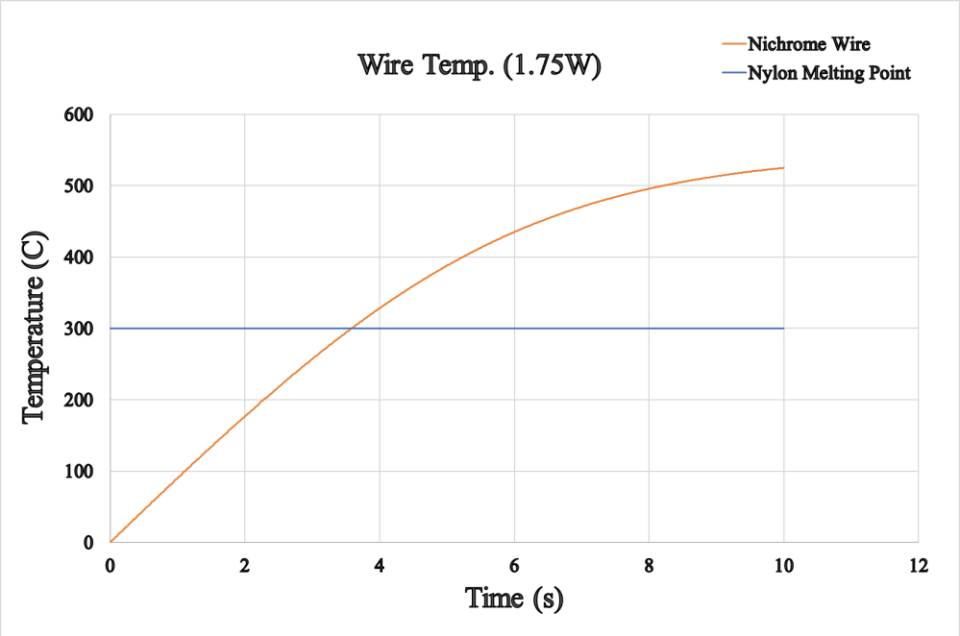


**Figure 23.** Nichrome Temperature Calculations

As seen in Figure 23 the nichrome wire exceeded the nylon rope's melting point and will cut the nylon. This was also down experimentally to verify that the nichrome wire would cut or melt the nylon at certain temperatures. The experiments performed were not performed in a vacuum, so convection did have an impact on the final temperature of the nichrome wire. The nichrome wire was supplied with power till it reached a steady state, at this time the temperature of the wire was constant. The nylon rope was then put into contact with the nichrome and the results were recorded. The team concluded that if the nichrome wire reached the melting point of the nylon rope the nylon rope would be cut.

The final step was to attach the HRM to the CubeSat. This was done by constructing pins that would attach to the CubeSat chassis and the panels. Two pins were inserted into the top of the chassis and one pin was placed onto the panel. The nylon rope was then wrapped around the three pins forming a triangle that will hold the array in the stowed configuration. The pins all have a notch placed in them to hold the nylon rope in place, this was done to prevent the nylon rope from slipping off and deploying the array early. The nichrome burn wire is coiled around the base of the nylon rope. It was found that the nichrome should be coiled around the nylon five times to ensure that there was a physical connection between the two. The HRM was then tested twenty times after being added to the CubeSat. The HRM successfully held and then released the panels all twenty

times during testing. 1.75W were provided to the nichrome wire during these tests and it took on average of 3 seconds for the wire to cut the nylon rope holding the panels. Although the tests were successful more tests are needed to prove the design. Two figures can be seen below of the testing. Figure 24 is in the stowed configuration, Figure 25 is the deployed configuration after the HRM cuts the nylon.

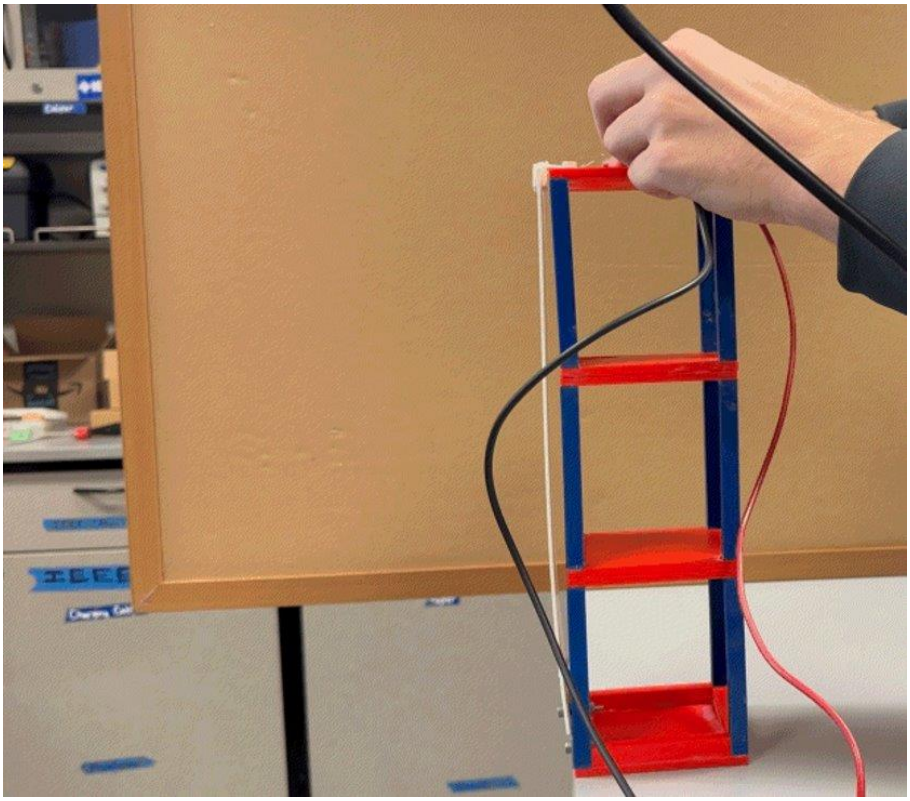

**Figure 24.** Testing Stowed Configuration.

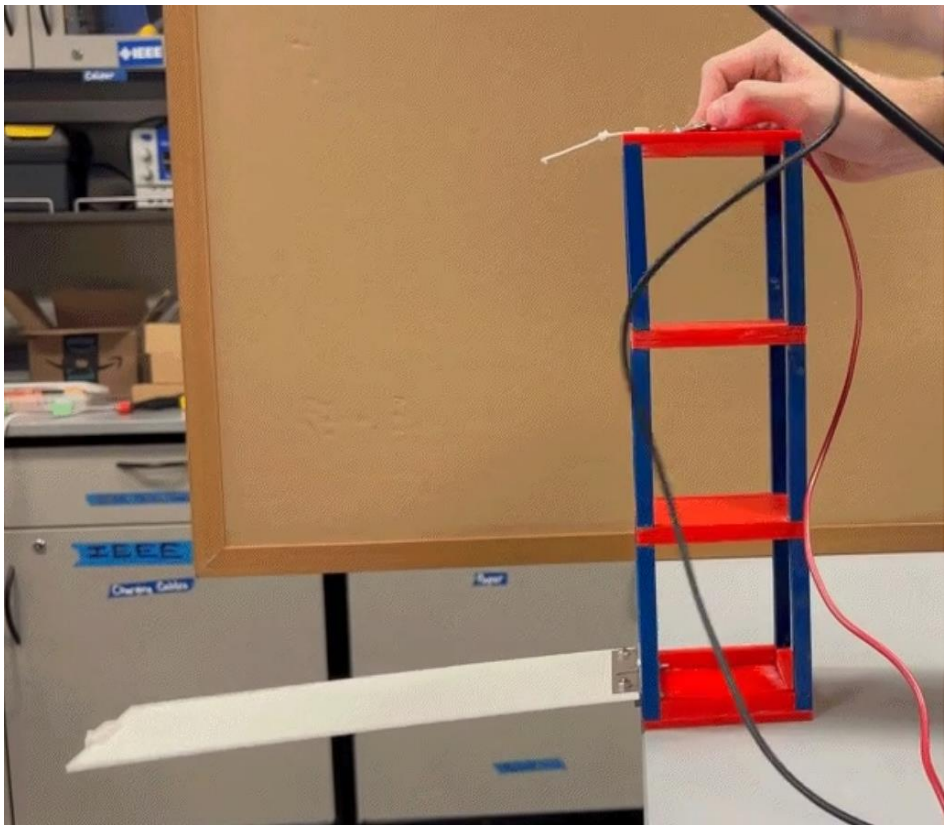

**Figure 25.** Testing Deployed Configuration.

# 4 DESIGN CONSIDERATIONS

## *4.1 PUBLIC SAFETY*

A public safety design factor was identified because of the potential risk a CubeSat introduces once deployed in space. These satellites being deployed in Low-Earth Orbit have been known to stay in orbit longer than the time they are allotted. This "space debris" becomes a risk to any future human spacecraft launch, as the debris could easily damage a spacecraft moving at high velocity [13]. This design factor was important to the project because it addresses the first fundamental canon of the Code of Ethics for Engineers [14]. The design of the deployable solar array is justified by acting as a drag mechanism to assist in the re-entry time of the CubeSat.

## *4.2 ECONOMIC FACTOR*

An economic factor was also identified which also related to the time the CubeSat stays in orbit. Another important reason that the CubeSat re-entry is time-dependent is because a license is issued to the team that built the CubeSat. This license permits the satellite to be in orbit, but only for a certain amount of time. After the given time, the license expires and must be renewed if the satellite is still in orbit and would cost the team thousands of dollars. This is what happened with the previous UNITE team's CubeSat deployment in 2019. The addition of the solar array would act as a drag mechanism to shorten the time for the satellite to re-enter the atmosphere.

Table 3 shows the complete bill of materials, including all 3D printed materials, and materials not used in the final prototype. An economic design factor was considered by utilizing 3D printing where applicable. This allowed for a much lower cost prototype than if the parts such as the chassis were to be fabricated from its intended material aluminum. This additionally saved any machining costs that may have been incurred in the fabrication process.

**Table 3.** Bill of Materials.

| **Budget** | **Quantity** | **Description** | **Unit Cost** | **Total** |
|---|---|---|---|---|
| | 4 | Torsional Hinge | $7 | $28 |
| | 1 | Nichrome Burn Wire | $5 | $5 |
| | 1 | 3D Printed Materials | $2 | $2 |
| | 1 | Nylon Rope | $5 | $5 |
| | 12 | Neodymium Magnet | $1.25 | $15 |
| | 1 | Steel Shim Stock | $19 | $19 |
| | 1 | Shipping | $31 | $31 |
| **Total** | | | | **$105** |

# 5 CONCLUSIONS AND RECOMMENDATIONS

## *5.1 CONCLUSION*

This report has presented a problem statement involving a deployable solar array for the future development of USI's CubeSat project. Following the problem statement was the description of the solution, which included the decision to determine the feasibility of a CORE joint and an HRM for CubeSat solar array deployment. This report presented the objective and deliverables followed by the justification of the project. These justifications were: the motivation and need, the engineering problems the team faced, analysis of previous solutions to the same problem, and the engineering knowledge required for the project.

The team has worked together to find the most viable solution for a deployable solar array for a 3U CubeSat. This solution was decided according to official regulations, team requirements, and engineering knowledge already obtained by the team members. A testable prototype has been built to support design choices and confirm the operation and reliability of the mechanism selected.

## *5.2 LESSONS LEARNED*

Important lessons learned from this project were the functionality of CORE joints, and the properties of Joule Heating within a nichrome wire. A deeper understanding of heat transfer was also needed to accurately calculate the temperature of the nichrome wire due to Joule Heating. The team recognized through testing that the flexures designed for CORE joints are purposed to function specifically as a revolute joint. This means that the joints are better suited for applications where a typical hinge can be used, rather than a torsional hinge purposed to supply a torque once deflected from its resting position.

## *5.3 DISPOSAL PLAN*

A disposal plan wouldn't be required for the mechanism if it were to be used on a future CubeSat deployment, since it would eventually burn up during re-entry. For the prototype however, the non-3D printed parts could be re-used for a later or final model of the mechanism. This includes the hinges, nichrome wire, and nylon rope. The 3D printed parts (dummy chassis, panels, CORE joint surfaces) may be recycled where they can be ground or formed into new products. A unique feature of PLA is that it is biodegradable in the right conditions, so it could also be broken down unlike many other thermoplastics. The parts not used in the final prototype

(steel shim stock, neodymium magnets) can also be properly disposed of. The steel can be sold for scrap while the magnets are recommended to be recycled since they aren't biodegradable. This can be done at a recycling center or electronics store that accepts them.

## *5.4 FUTURE RECOMMENDATIONS*

The following recommendations have been made for the UNITE team regarding the deployable solar array:

- Vacuum chamber deployment testing

A deployment test in a vacuum chamber would more accurately simulate the HRM in space, as there would be no heat transfer due to convection, only conduction and radiation.

- PCB design and fabrication

While the testing for this project was all performed with a power supply at constant amperage, this isn't completely accurate. If this mechanism were to be used on a future CubeSat project, a PCB design would be required to allow for remote actuation of the HRM to initiate deployment. The PCB design must also incorporate a feature that only allows the mechanism to deploy "a minimum of 30 minutes after the CubeSat's deployment switch(es) are activated during dispenser ejection" [1]. A project that utilized a similar HRM has been included in literature review that included the fabrication of a PCB that allowed for this actuation of panels on all four lateral sides [5].

## REFERENCES


1 *Static1.Squarespace.com*. https://static1.squarespace.com/static/5418c831e4b0fa4ecac1bacd/t/62193b7fc9e72e0053f00910/1645820809779/CDS+REV14_1+2022-02-09.pdf.

2 Kissel, G. (2019). (rep.). *UNITE CubeSat: From Inception to Early Orbital Operations*. Evansville, IN: University of Southern Indiana.

3 McGill, Eric. *Development of a Self-Orienting CubeSat Solar Array*. University of Dayton, 2018.

4 Santoni, Fabio & Piergentili, Fabrizio & Donati, Serena & Perelli, Massimo & Negri, Andrea & Marino, Michele. (2014*). An innovative deployable solar panel system for Cubesats.* Acta Astronautica. 95. 210–217. 10.1016/j.actaastro.2013.11.011.

5 Bhattarai, Shankar, et al. "Development of Pogo Pin-Based Holding and Release Mechanism for Deployable Solar Panel of CubeSat." *International Journal of Aerospace Engineering*, Hindawi, 5 May 2019, https://doi.org/10.1155/2019/2580865.

6 Howell, Larry. *Compliant Mechanisms*. Hoboken, NJ, United States, Wiley, 2001.

7 Halverson, Peter Andrew. "Multi-Stable Compliant Rolling-Contact Elements." *BYU ScholarsArchive*, https://scholarsarchive.byu.edu/etd/895/.

8 "Material Properties." *Marlow Ropes*, 30 Aug. 2023, www.marlowropes.com/innovation/material-properties/.

9 "Alloy 650 (Nichrome 80)." *Pelican Wire*, 16 Sept. 2021, pelicanwire.com/alloy/alloy-650-2/.

10 Dye, C. (2023, May). *A Systematic Study into The Design and Utilization of Burn Wire as a Means of Tensioning and Releasing Spacecraft Mechanisms Through Applied Joule Heating* (thesis). *scholarworks.uark.edu*. University of Arkansas. Retrieved October 2023, from https://scholarworks.uark.edu/cgi/viewcontent.cgi?article=1120&context=meeguht.

11 Bryson, Paul. “Heating a Nichrome Wire with Math .” *Brysonics*, 18 May 2018, www.brysonics.com/heating-a-nichrome-wire-with-math/.

12 Paul , James, et al. Nasa.Gov, *CubeSat On-Orbit Temperature Comparison to Thermal-Balance-Tuned Model Predictions*, CubeSat On-Orbit Temperature Comparison to Thermal-Balance-Tuned Model Predictions. Accessed Oct. 2023. https://s3vi.ndc.nasa.gov/ssri-kb/static/resources/Thermal_Balance_Paper_Rev4.pdf

13 Ostrom, Chris L, and John N Opiela. *Orbital Debris Mitigation and CUBESATS - European Space Agency*, conference.sdo.esoc.esa.int/proceedings/sdc8/paper/143/SDC8-paper143.pdf. Accessed 5 Dec. 2023.

14 *Code of Ethics for Engineers - National Society of Professional Engineers*, www.nspe.org/sites/default/files/resources/pdfs/Ethics/CodeofEthics/NSPECodeofEthicsforEngineers.pdf. Accessed 14 Nov. 2023.

# APPENDIX

Appendix A:  Schedule

Appendix B:  Bill of Materials

Appendix C:  Requirements

Appendix D:  Mass Table (with margin)

Appendix E:  Design Considerations and Standards (students - see "Appendix N" in Blackboard site for attachment.)

Appendix F: Concept of Operations

Appendix G: Two Failure Modes and Effects Analyses

Appendix H: Mechanical Block Diagram

Appendices

A. Schedule

**Table 4.** Schedule

| | |
|---|---|
| Proposal First Draft | 2/17/2023 |
| Proposal Final Proposal | 2/24/2023 |
| Design Proposal Oral Presenation | 3/13/2023 |
| Preliminary Design Review Presentation | 4/10/2023 |
| Pre-Senior Design Report | 4/26/2023 |
| Arrange weekly advisor meeting | 8/21/2023 |
| Critical Design Review | 9/21/2023 |
| Order hardware | 9/22/2023 |
| Design Presentation Reviews Complete | 11/10/2023 |
| Senior Design Report Draft Due to Advisor | 11/17/2023 |
| Final Senior Design Presentation | 12/1/2023 |
| Senior Design Poster Session | 12/7/2023 |
| Final Senior Design Report Due to Advisor | 12/8/2023 |

| | |
|---|---|
| Final Design Report submitted to SOAR | 12/18/2023 |

B. Bill of Materials

**Table 5.** Bill of Materials

| **Budget** | **Quantity** | **Description** | **Unit Cost** | **Total** |
|---|---|---|---|---|
| 1) | 4 | Torsional Hinge | $7 | $28 |
| 2) | 1 | Nichrome Burn Wire | $5 | $5 |
| 3) | 1 | Dummy Chassis | $2 | $2 |
| 4) | 1 | Nylon Rope | $5 | $5 |
| 5) | 12 | Neodymium Magnet | $1.25 | $15 |
| 6) | 1 | Steel Shim Stock | $19 | $19 |
| 7) | 1 | Shipping | $31 | $31 |
| **Total** | | | | **$105** |

C. Requirements

- The deployable solar array:

1. Shall be within the dimensions of the CubeSat standards (100×100×340.5)mm
2. Shall deploy four arms that carry solar panels
3. Shall not release any components from the CubeSat at any time
4. Shall not damage the other components of the CubeSat
5. Shall be developed as a testable prototype
6. Shall deploy to a specific angle (90°)

D. Mass Table (with margin)

**Table 6.** Mass Table

| Item No. | Item | Mass (kg) | Quantity | Total (kg) |
|---|---|---|---|---|
| 1 | Solar Panel | ~0.060 | 4 | 0.18 |
| 2 | Torsional Hinge | ~0.002 | 8 | 0.016 |
| 3 | HRM | ~0.01 | 4 | 0.04 |
| | | | **Total:** | **0.356** |

E. Design Considerations and Standards

**Table 7.** Design Factors

| Design Factor | Page number, or reason not applicable |
|---|---|
| Public health safety, and welfare | 34 |
| Global | N/A |
| Cultural | N/A |
| Social | N/A |
| Environmental | N/A |
| Economic | 34 |
| Ethical & Professional | N/A |
| Reference for Standards | 34 |

F. Concept of Operations

A. Deployment of CubeSat from larger shuttle

B. Deployment of solar array 30 minutes after release of CubeSat

a. Burn wire initiation

b. Panels rotate about hinge mechanism, deploy to stable position

C. Solar array power generation

D. Re-entry into atmosphere

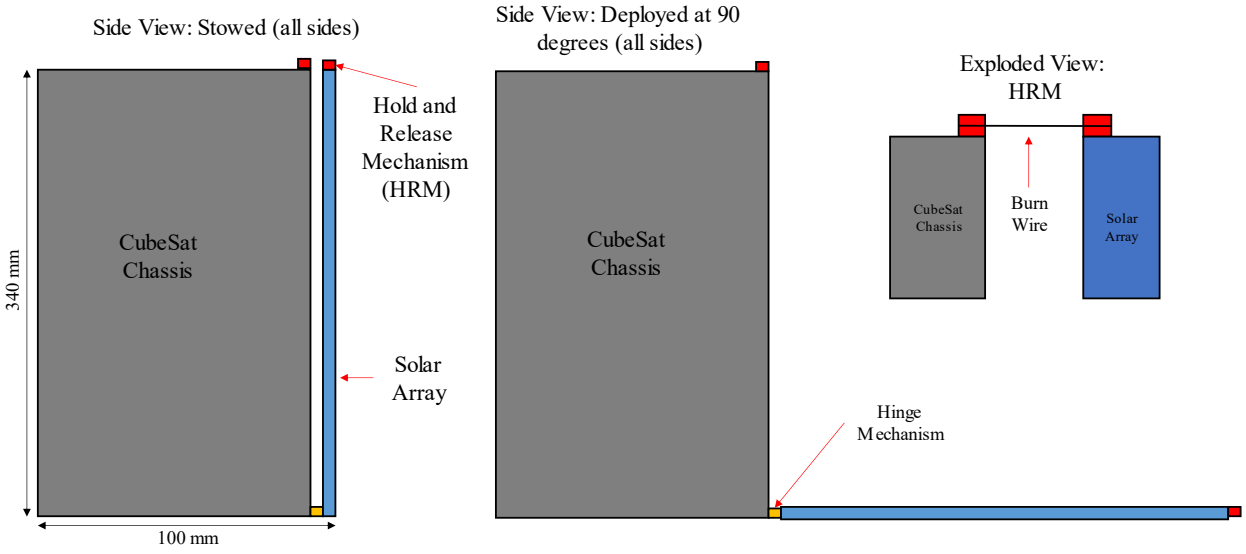


**Figure 26.** Concept of Operations.

G. Two Failure Modes and Effects Analysis

**Table 8.** FMEA

| Item | Failure Modes | Cause of Failure | Possible Effects | Level | Possible action to reduce failure rate or effects |
|---|---|---|---|---|---|
| Hold and Release Mechanism | Array doesn't deploy | Incorrect Calculation/Design Incorrect Handling/Transportation | CubeSat remains in orbit too long | High | Confirm correct calculations and design. Also confirm any manufacturing process was performed correctly |
| Hinge Mechanism | Array doesn't deploy properly | Vibrations, Incorrect Calculation/Design | Appropriate amount of power isn't generated | High | Perform multiple tests on the deployment of the array to confirm it fully and correctly deploys |

H. Mechanical Block Diagram

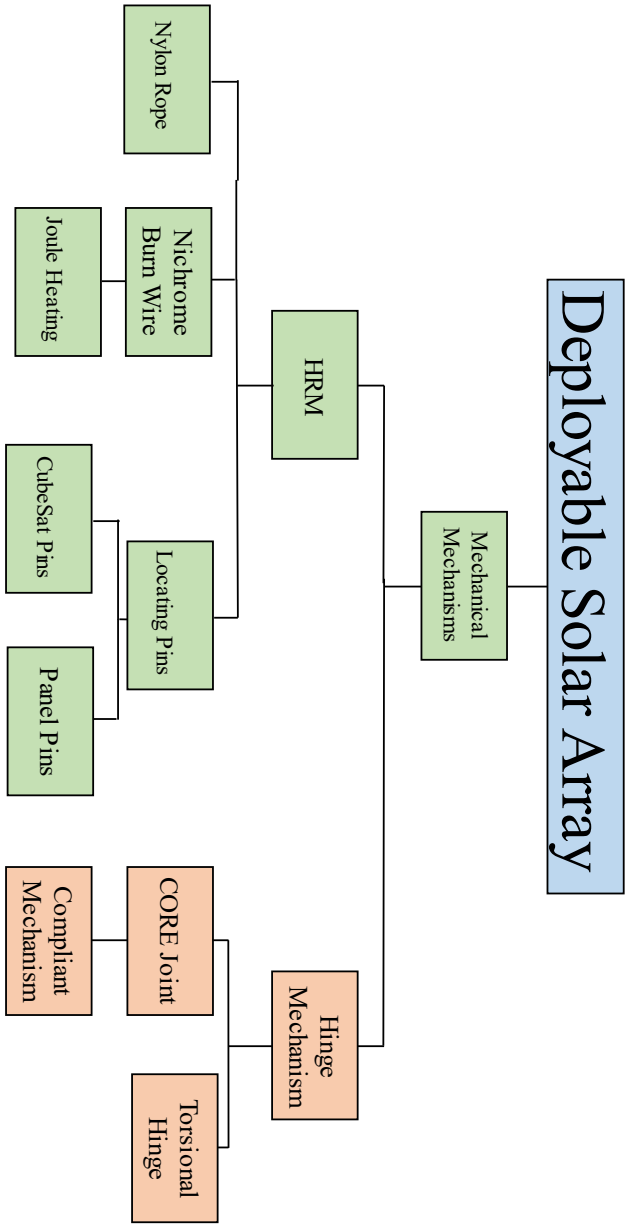


**Figure 27.** Mechanical Block Diagram